Temperature and vegetation seasonality diminishment over northern lands

L. Xu[1]★†, R. B. Myneni[1]★†, F. S. Chapin III[2], T. V. Callaghan[3,4], J. E. Pinzon[5], C. J. Tucker[5], Z. Zhu[1], J. Bi[1], P. Ciais[6], H. Tømmervik[7], E. S. Euskirchen[2], B. C. Forbes[8], S. L. Piao[9,10], B. T. Anderson[1], S. Ganguly[11], R. R. Nemani[12], S. J. Goetz[13], P. S. A. Beck[13], A. G. Bunn[14], C. Cao[15,16] and J. C. Stroeve[17]

Global temperature is increasing, especially over northern lands (>50° N), owing to positive feedbacks[1]. As this increase is most pronounced in winter, temperature seasonality (S_T)—conventionally defined as the difference between summer and winter temperatures—is diminishing over time[2], a phenomenon that is analogous to its equatorward decline at an annual scale. The initiation, termination and performance of vegetation photosynthetic activity are tied to threshold temperatures[3]. Trends in the timing of these thresholds and cumulative temperatures above them may alter vegetation productivity, or modify vegetation seasonality (S_V), over time. The relationship between S_T and S_V is critically examined here with newly improved ground and satellite data sets. The observed diminishment of S_T and S_V is equivalent to 4° and 7° (5° and 6°) latitudinal shift equatorward during the past 30 years in the Arctic (boreal) region. Analysis of simulations from 17 state-of-the-art climate models[4] indicates an additional S_T diminishment equivalent to a 20° equatorward shift could occur this century. How S_V will change in response to such large projected S_T declines and the impact this will have on ecosystem services[5] are not well understood. Hence the need for continued monitoring[6] of northern lands as their seasonal temperature profiles evolve to resemble those further south.

The Arctic (8.16 million km²) is defined here as the vegetated area north of 65° N, excluding crops and forests, but including the tundra south of 65° N. The boreal region (17.86 million km²) is defined as the vegetated area between 45° N and 65° N, excluding crops, tundra, broadleaf forests and grasslands south of the mixed forests, but including needleleaf forests north of 65° N (Supplementary Fig. S1). These definitions are a compromise between ecological and climatological conventions. Importantly, they include all non-cultivated vegetation types within these two regions.

Comparisons of changes in seasonality of physical and biological variables require definitions that are concordant, have an ecological underpinning, for example, vegetation photosynthetic activity in the north depends on the seasonal cycle of temperature and not on the difference between annual maximum and minimum temperatures, and satisfy the principle that seasonality increases with latitude at an annual timescale owing to patterns of insolation resulting from Sun–Earth geometry alone (Fig. 1a and Supplementary Information S2.A). Therefore, S_T is defined as $[1 \div \overline{T}_{yr}(l)]$, where $\overline{T}_{yr}(l)$ is the zonally averaged annual mean temperature at latitude l. S_V is analogously defined as $[1 \div \overline{N}_p(l)]$, where $\overline{N}_p(l)$ is the zonal mean of photosynthetic activity averaged over the photosynthetically active period (PAP) at latitude l. These definitions possess the above-mentioned attributes and accurately represent the respective seasonal cycles (Supplementary Information S2.A.3).

The latitudinal profiles of PAP-mean temperature from 50° N to 75° N (ice sheets excluded throughout) show warming of 1–2 °C between the early 1980s and late 2000s (Fig. 1b). Analogous profiles of normalized difference vegetation index (NDVI), a proxy for vegetation photosynthetic activity[3], show a similar increase. S_V is tightly coupled to S_T in the north (Fig. 1c). The slope of this relationship (β_{VT}) has not changed in the past 30 years (Fig. 1c, inset). Figure 1b,c may thus indicate widespread and matching patterns of temperature and NDVI increase and corresponding reductions in S_T and S_V throughout northern lands. If this were to continue, significant increases in productivity may be expected in the boreal/Arctic region during this century on the basis of climate model projections of large S_T diminishment, even as insolation seasonality remains unchanged[7], which would have major ecological, climatic and societal impacts. This apparent constancy of β_{VT} in Fig. 1c is tested in four ways.

In the first test, the constancy of β_{VT} is based on widespread statistically significant increases in PAP-mean NDVI and

[1]Department of Earth and Environment, Boston University, Boston, Massachusetts 02215, USA, [2]Institute of Arctic Biology, University of Alaska Fairbanks, Fairbanks, Alaska 99775, USA, [3]Royal Swedish Academy of Sciences, PO Box 50005, 104 05 Stockholm, Sweden, [4]Department of Animal and Plant Sciences, University of Sheffield, Western Bank, Sheffield S10 2TN, UK, [5]Biospheric Sciences Branch, NASA Goddard Space Flight Center, Greenbelt, Maryland 20771, USA, [6]Laboratoire des Sciences du Climat et de l'Environnement, CEA-CNRS-UVSQ, 91191 Gif sur Yvette, Cedex, France, [7]Norwegian Institute for Nature Research, Fram-High North Research Center for Climate and the Environment, N-9296 Tromsø, Norway, [8]Arctic Centre, University of Lapland, FI-96101 Rovaniemi, Finland, [9]Department of Ecology, Peking University, Beijing 100871, China, [10]Institute of Tibetan Plateau Research, Chinese Academy of Sciences, Beijing 100085, China, [11]Bay Area Environmental Research Institute, NASA Ames Research Center, Moffett Field, California 94035, USA, [12]NASA Advanced Supercomputing Division, Ames Research Center, Moffett Field, California 94035, USA, [13]The Woods Hole Research Center, Woods Hole, Falmouth, Massachusetts 02540, USA, [14]Department of Environmental Sciences, Huxley College, Western Washington University, Bellingham, Washington 98225, USA, [15]State Key Laboratory of Remote Sensing Science, Institute of Remote Sensing and Digital Earth, Chinese Academy of Sciences, Beijing 100101, China, [16]School of Resource and Environment, University of Electronic Science and Technology of China, Chengdu, Sichuan 611731, China, [17]National Snow and Ice Data Center, University of Colorado, Boulder, Colorado 80309, USA. †These authors contributed equally to this work. *e-mail: xuliang@bu.edu; ranga.myneni@gmail.com.
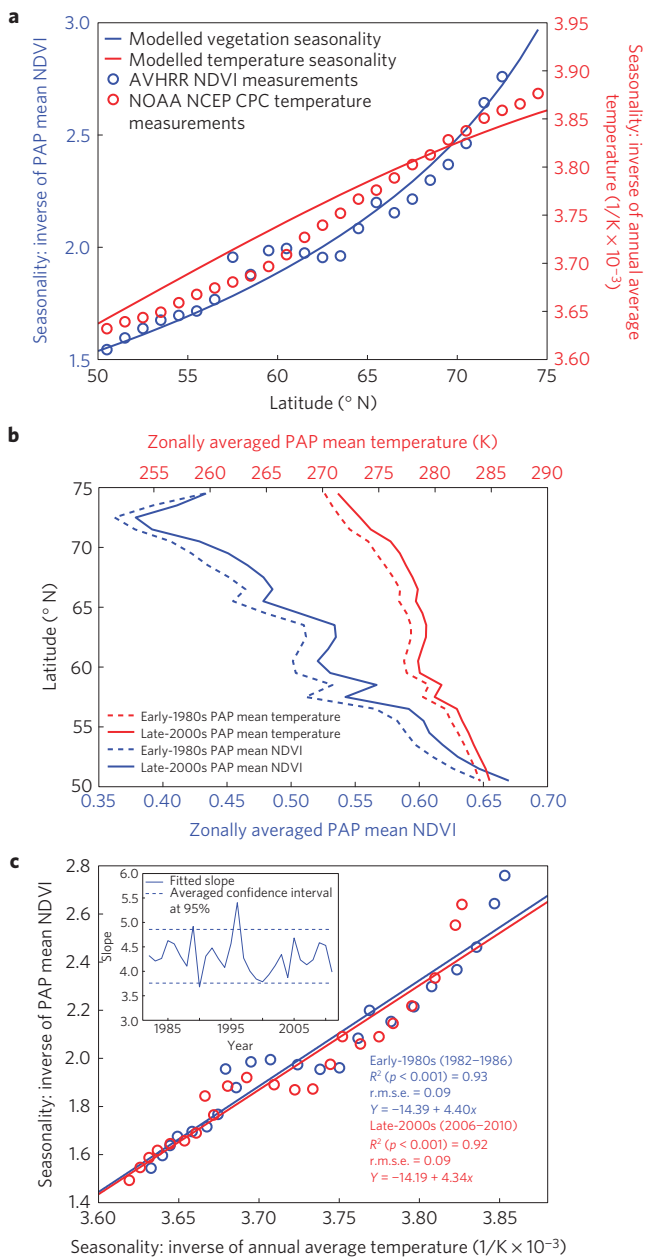
Figure 1 | Latitudinal and temporal variation of temperature and vegetation seasonality (S_T and S_V). a, Comparison of model-predicted S_T and S_V (solid lines; Supplementary Information S2.A) with data for the period 1982–1986. **b**, Latitudinal profiles of zonally averaged PAP-mean temperature (red) and NDVI (blue). The periods early 1980s and late 2000s refer to years 1982–1986 and 2006–2010. **c**, Relationship between S_T and S_V for two time periods. The inset shows year-to-year variation in the slope of this relationship and the dashed lines represent 95% confidence intervals. NOAA NCEP CPC temperature and AVHRR NDVI3g data over the Arctic and boreal regions (Supplementary Fig. S1) were used. NOAA, National Oceanic and Atmospheric Administration; NCEP, National Centers for Environmental Prediction; CPC, Climate Prediction Centre; AVHRR, Advanced Very High Resolution Radiometer; NDVI3g, third generation Normalized Difference Vegetation Index.

temperature. This is assessed using four statistical models. Results from two statistically robust models are mainly discussed here (Models 3 and 4 in Supplementary Information S2.C.1).

Regarding PAP-mean NDVI ($\overline{N}_P$), three points are noteworthy. First, the proportion of Arctic vegetation with a statistically significant ($p < 0.1$) increase in $\overline{N}_P$ (greening) varied from 32 to 39% and the proportion with a statistically significant decrease in $\overline{N}_p$ (browning) was <4%. In the boreal region, greening varied from 34 to 41% and browning was <5%. The ratio of greening to browning proportion is even higher at $p < 0.05$ in both regions (Supplementary Tables S2 and S3).

Second, the greening is most prominently seen in coastal tundra[8] and eastern mixed forests in North America, needleleaf and mixed forests in Eurasia, and shrublands and tundra in Russia (Fig. 2a and Supplementary Fig. S7). North American boreal vegetation shows a fragmented pattern of greening and browning[9,10], unlike its counterpart in Eurasia, which shows widespread contiguous greening. Further analysis reveals little evidence of widespread browning of boreal vegetation at the circumpolar scale (Supplementary Information S3.A).

Third, about 90% of the Arctic and 70% of the boreal greening vegetation show $\overline{N}_P$ increases >2.5% per decade (Fig. 2c). These changes in $\overline{N}_P$ can be expressed as changes in PAP duration. For example, a trend of $+x$ days per decade at a location in Fig. 2b means that the vegetation there would require x more days of PAP in 1982, the first year of the NDVI record, to equal its $\overline{N}_P$ ten years later. About 88% of the Arctic and 81% of the boreal greening vegetation show extensions in PAP > 3 days per decade (Fig. 2d). These extensions hint of S_V declines in these two regions—this is further explored in the fourth test below.

Next, regarding temperature changes, PAP-mean temperature could not be accurately evaluated because of the coarse temporal resolution of temperature data (monthly). Therefore, statistical analysis was performed on a per-pixel basis but using a close analogue, May–September (warm-season) average temperature, $\overline{T}_{WS}$. The proportion of Arctic and boreal regions exhibiting statistically significant increase in $\overline{T}_{WS}$ varied from 51 to 54% (Supplementary Table S4 under the heading Significant Trends; Supplementary Fig. S8). The proportion exhibiting statistically significant decrease in $\overline{T}_{WS}$ was <0.6%.

Therefore, the constancy of β_{VT} is based on widespread statistically significant increases in PAP-mean NDVI (34–41%) and its temperature analogue $\overline{T}_{WS}$ (51–54%) in the study area.

In the second test, the constancy of β_{VT} is based on spatially matching statistically significant changes in $\overline{N}_P$ and $\overline{T}_{WS}$. The sign of significant trends in $\overline{N}_P$ and $\overline{T}_{WS}$, or lack of such trends, is similar in about 47% of the Arctic and boreal vegetated lands (Fig. 3a,b; all model results in Supplementary Fig. S9 and Table S4). The trends of $\overline{N}_P$ and $\overline{T}_{WS}$ are of opposite sign in <2% of the study area. Greening or browning is not observed in an additional 27–31% of vegetated lands where warming is moderate. This pattern is seen in evergreen needleleaf forests of eastern North America, deciduous needleleaf forests of Russia and in patches in western Canada and Alaska. Thus, in 74–78% of the Arctic and boreal regions, trends in $\overline{N}_P$ and $\overline{T}_{WS}$ did not strongly oppose one another during the past 30 years. Therefore, the constancy of β_{VT} is based on spatially matching statistically significant changes in $\overline{N}_P$ and $\overline{T}_{WS}$.

In the third test, β_{VT} is spatially invariant, that is coefficients β_{VT} of the Arctic and boreal region are similar. Statistical analysis with two regression models[9] indicates highly significant ($p < 0.01$) relationships between S_V and S_T anomaly time series in both regions (Fig. 3c,d and Supplementary Table S5). Here, S_T is defined in terms of PAP-mean temperature for large zonal bands such that it satisfies the Sun–Earth geometric definition of seasonality. The coefficients associated with the temperature variable of the two regions are statistically similar in both models. Therefore, β_{VT} is spatially invariant over the 30-year study period.

In the fourth test, β_{VT} is spatially and temporally invariant, that is, coefficients β_{VT} of the Arctic and boreal regions are not only similar but also did not change between the first and second halves of the 30-year study period. To avoid performing statistical analysis
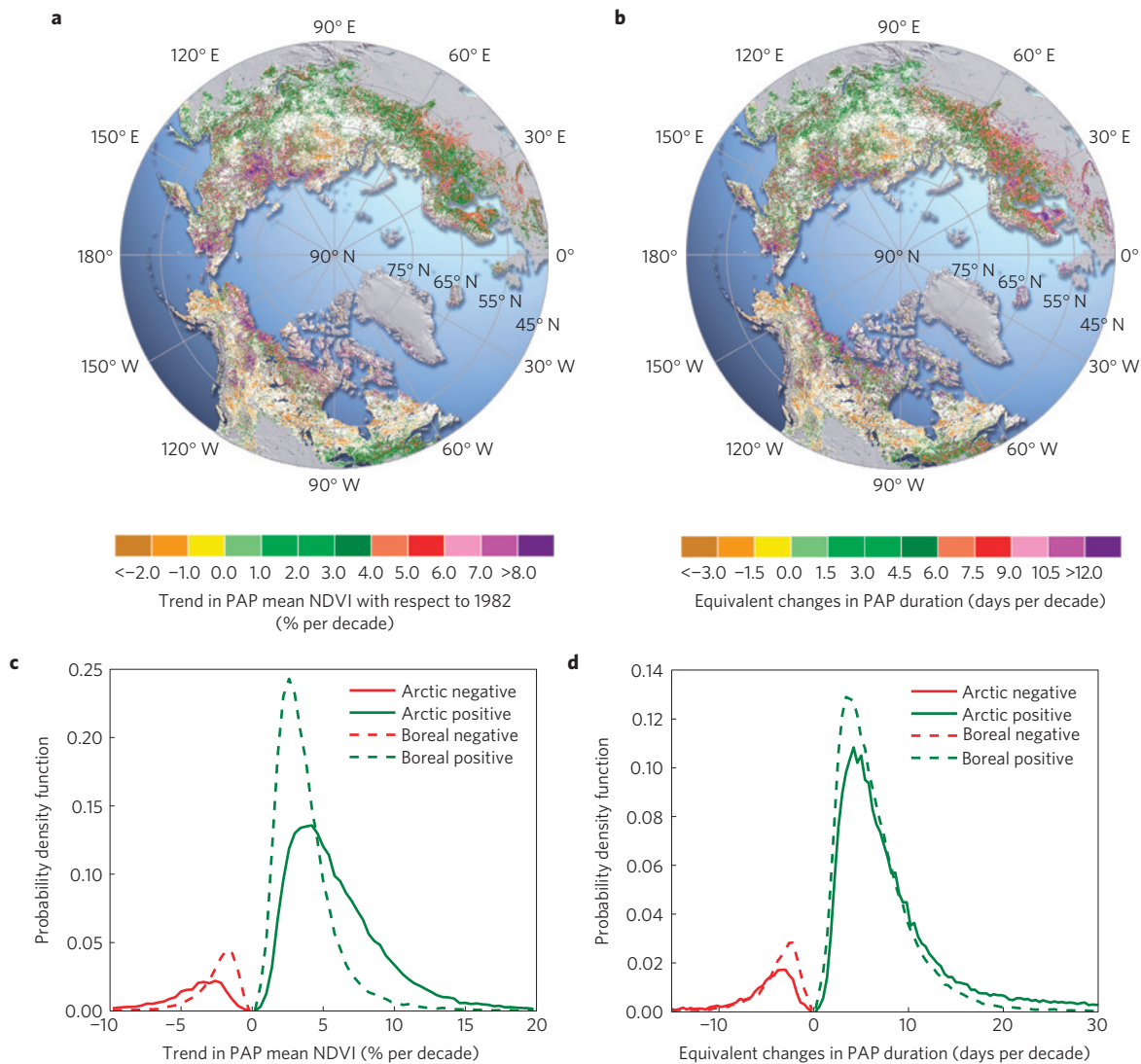
Figure 2 | Spatial patterns of changes in vegetation photosynthetic activity. a, Trends in PAP-mean NDVI, $\overline{N}_P$. **b,** Trends in equivalent changes in PAP duration, E. **c,d,** The probability density functions of $\overline{N}_P$ and E. Areas showing statistically significant ($p < 0.1$) trends from statistical Model 3 (ARIMA($p,1,q$), $p = 1, 2$; $q = 1, 2$) are coloured in **a,b.** Areas with statistically insignificant trends are shown in white colour. Grey areas correspond to lands not considered in this study. Similar maps for $\overline{N}_P$ trends from all four statistical models are shown in Supplementary Fig. S7. Equivalent changes in PAP duration, $E(p,y)$ of pixel p in year shown in **b** are evaluated as $[A(p,y) \div A(p,1982)] \times \mathrm{PAP}(p) - \mathrm{PAP}(p)$, where A is PAP-mean NDVI. Let $x(p)$ denote the trend in $A(p)$ per year with respect to 1982, the first year of the NDVI data series. Thus, in year 1, $E(p,1982) = E_0(p) = 0$. In year 2, $E(p,1983) = E_1(p) = \{A_0(p) \times [1 + x(p)]\} \div A_0(p) \times \mathrm{PAP}(p) - \mathrm{PAP}(p)$. The trend in $E(p) = E_1(p) - E_0(p) = x(p) \times \mathrm{PAP}(p)$. Note that NDVI are PAP-independent measurements. Therefore, the patterns in **a,b** are different.

on short data records, changes in S_T and S_V were translated into latitudinal shifts during each half of the study period and compared with one another. Briefly, data from the early part of the time series were used to define baselines depicting seasonality variation with respect to latitude in the Arctic and boreal regions. The location of temperature and vegetation seasonality on the respective baselines for three periods yielded seasonality declines in terms of latitude between the first half (mid 1990s and early 1980s) and second half (late 2000s and mid 1990s) of the data record.

The early-1980s (1982–1986) Arctic warm-season S_T corresponded to the warm-season S_T of vegetated lands >64.8° N (Fig. 4a). By the late 2000s, the warm-season temperature profile of the Arctic was similar to the early-1980s warm-season temperature profile of vegetated lands >60.8° N—a decline in S_T of 4.0° in latitude. The early-1980s boreal region warm-season S_T corresponded to the warm-season S_T of vegetated lands between 45° N and 66.1° N. By the late 2000s, the warm-season temperature

profile of the boreal region was similar to the early-1980s warm-season temperature profile of vegetated lands between 45° N and 60.9° N—a decline in S_T of 5.2° in latitude. Changes in S_V were similarly quantified (Fig. 4b). The corresponding declines in Arctic and boreal S_V are 7.1° and 6.3° in latitude.

The difference in S_T decline between the first and second halves of the 30-year period is negligible in both the Arctic and boreal region, in view of the coarse resolution of temperature data. However, this is not the case with S_V. The Arctic S_V decline accelerated, that is, the greening rate increased over time, from 2.15° latitude between the early 1980s and mid 1990s to 4.9° latitude between the mid 1990s and late 2000s. In contrast, S_V decline in the boreal region decelerated from 5.7° to 0.6° latitude. These varying rates of S_V declines are inconsistent with the idea of a spatially and temporally invariant β_{VT}.

In summary, the first three tests support the observed (Fig. 1c) tight coupling between S_V and S_T. However, the fourth test
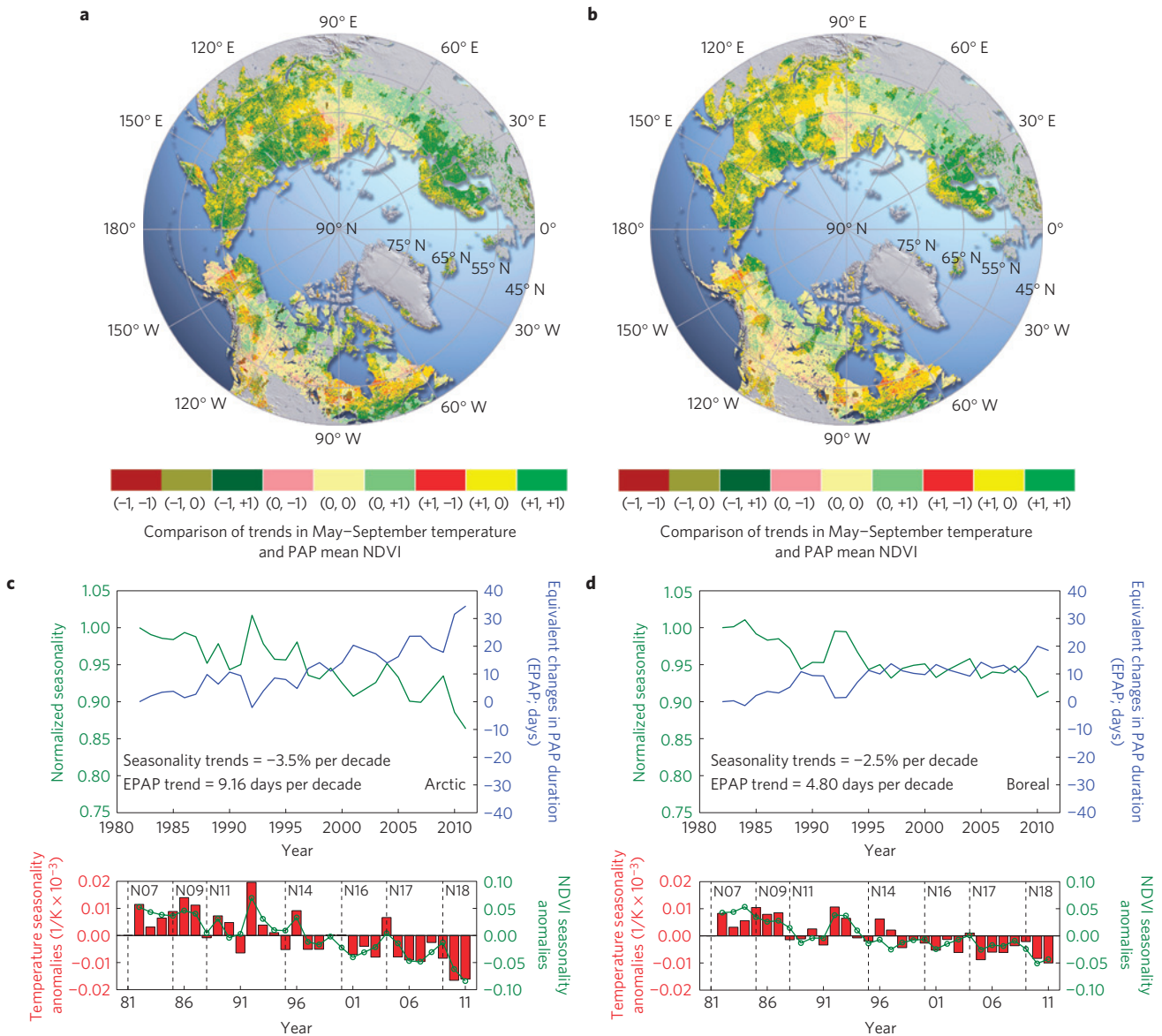
Figure 3 | Relationship between temperature and vegetation seasonality (S_T and S_V). a, Comparison of trends of May–September (warm-season) average temperature, $\overline{T}_{WS}$, and PAP-mean NDVI, $\overline{N}_p$. Statistically significant ($p < 0.1$) positive trends are denoted as +1, negative trends as −1 and insignificant trends as 0. The first character in each pair below the colour bar denotes $\overline{T}_{WS}$ trend and the second character denotes $\overline{N}_p$ trend. Statistical Model 3 (ARIMA(p, 1, q), $p = 1, 2$; $q = 1, 2$) was used to assess statistical significance and trend magnitudes. Temperature data were downscaled to the spatial resolution of NDVI data using the method of nearest-neighbour interpolation. As this may potentially create artefacts, only the changes in sign of the respective trends are compared. **b**, The same as in **a** but using Vogelsang's $t - PS_T$ method. Grey areas correspond to lands not considered in this study. Similar maps from all statistical models are shown in Supplementary Fig. S9. **c**, Time series of Arctic S_V with respect to S_V in year one (1982) of the NDVI data series and corresponding equivalent changes in PAP duration. These time series are from pixels exhibiting statistically significant trends in $\overline{N}_p$ as determined by statistical Model 3 (Fig. 2a). The lower panels show S_T and S_V anomaly time series (statistics in Supplementary Table S5). The dates of different AVHRR sensors are indicated as N07 (NOAA 7), N09 (NOAA 9) and so on. **d**, The same as in **c** but for the boreal region. NOAA NCEP CPC temperature data were used.

indicates that β_{VT} varies with time and that this variation differs between the Arctic and boreal regions, with greening in the Arctic accelerating over time, whereas boreal greening is decelerating over time. The robustness of these conclusions is addressed in Supplementary Information S3.B.

Empirical evidence suggests that in addition to direct effects of warming[11,12] several other factors influence β_{VT} (refs 13–15). These include: warming-induced disturbances and recovery (summertime droughts[16], mid-winter thaws[17], increased frequency of fires and outbreaks of pests[18], shrinking and draining of lakes from thawing permafrost[19], desiccation of ponds[20],

colonization of the growing banks by vegetation[21] and so on), interacting effects of temperature and precipitation[22], complex feedbacks (feedbacks that enhance wintertime snow amount on land asymmetrically between Eurasia and North America[23], feedbacks from declining snow-cover extent on land[1] leading to longer growing seasons[3,9] and promoting vegetation compositional/structural changes[12,13,24,25], enhanced nitrogen mineralization in warmer soils insulated by increased shrub cover[26] and so on), anthropogenic influences (pollution from metal smelters[27], herding practices of grazing herbivores[28] and so on) and changes in wild herbivore populations[29]. These factors could have
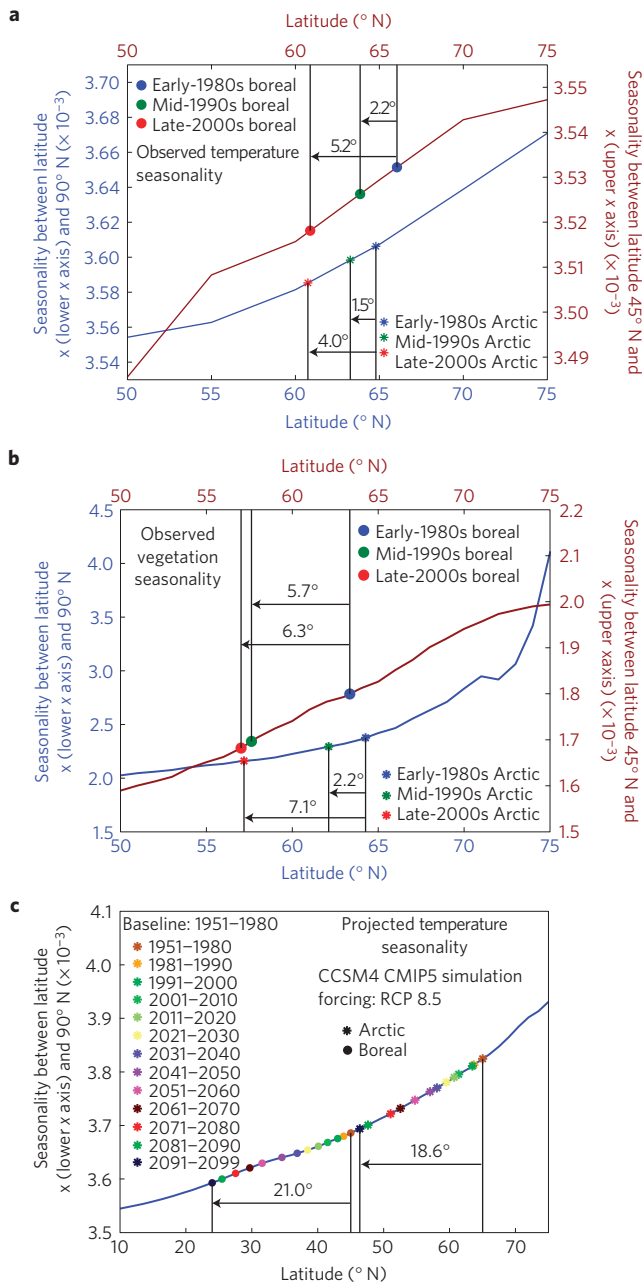
Figure 4 | Historical and projected seasonality declines. a, Observed diminishment of Arctic and boreal temperature seasonality. Note that S_T defined in terms of warm-season (May–September) average temperature, $S_T = [1 \div \overline{T}_{WS}]$, for large-zonal bands, for example, Arctic and boreal, satisfies the Sun–Earth geometric definitions of S_T (Supplementary Information S2.A) . The early 1980s, mid 1990s and late 2000s correspond to periods 1982–1986, 1995–1997 and 2006–2010. CRUTEM4 temperature data were used. **b**, The same as in **a** but for observed vegetation seasonality. **c**, Projection of temperature seasonality decline in the Arctic (asterisks) and boreal (dots) regions by the NCAR CCSM4 coupled model forced with Representative Concentration Pathway 8.5 (ref. 30) as a contribution to CMIP5 (ref. 4) activities. The declines inferred from 17 CMIP5 model simulations are given in Supplementary Table S6.

contributed to an amplification of β_{VT} in the Arctic and dampening in the boreal region.

Projections of S_T changes during this century are of interest given the observed relationship between S_V and S_T of the past

30 years. The median S_T decline in the Arctic and boreal regions from 17 climate models is 22.5° and 21.8° latitude by the decade 2091–2099 relative to the base period 1951–1980[4,30] (Supplementary Table S6)—example in Fig. 4c. That is, the annual temperature profile of the Arctic (boreal) during the base period 1951–1980 was similar to the annual temperature profile of lands north of 64.9° N (45.2° N). By 2091–2099, the annual temperature profile of the Arctic (boreal) is projected to be similar to the baseperiod annual temperature profile of lands north of 42.4° N (23.4° N).

The observed S_T decline during 2001–2010 is already greater than the multi-model median estimate (Supplementary Table S6). Recent trends are thus consistent with longer-term observations. The way that S_V will respond to large projected declines in S_T is largely unknown and depends on the adaptability of extant species and migration rates of productive southerly species in the face of unchanging insolation seasonality[7], increased frequency of winter warming events[17] and other factors (Supplementary Information S3.C). Such uncertainty is a strong argument in favour of continued monitoring[6] of northern lands as their seasonal temperature profiles evolve to resemble those further south.

Methods

All satellite and ground data used in this research are described in Supplementary Information S1. The derivation, testing and justification of temperature and vegetation seasonality definitions are described in Supplementary Information S2.A. The method for estimation of PAP is described in Supplementary Information S2.B. The four statistical methods employed to assess statistical significance and magnitude of trends are described in Supplementary Information S2.C. The evaluation of temperature and vegetation seasonality baselines and diminishment over time are described in Supplementary Information S2.D–S2.G.

References

1. Serreze, M. C. & Barry, R. G. Processes and impacts of Arctic amplification: A research synthesis. *Glob. Planet. Change* **77,** 85–96 (2011).
2. Mann, M. E. & Park, J. Greenhouse warming and changes in the seasonal cycle of temperature: Model versus observations. *Geophys. Res. Lett.* **23,** 1111–1114 (1996).
3. Myneni, R. B., Keeling, C. D., Tucker, C. J., Asrar, G. & Nemani, R. R. Increased plant growth in the northern high latitudes from 1981 to 1991. *Nature* **386,** 698–702 (1997).
4. Taylor, K. E., Stouffer, R. J. & Meehl, G. A. An overview of CMIP5 and the experiment design. *Bull. Am. Meteorol. Soc.* **93,** 485–498 (2012).
5. Chapin, F. S. *et al.* in *Ecosystems and Human Well-being: Current State and Trends* 717–743 (Island Press, 2005).
6. Post, E. *et al.* Ecological dynamics across the arctic associated with recent climate change. *Science* **325,** 1355–1358 (2009).
7. Hays, J. D., Imbrie, J. & Shackleton, N. J. Variations in the Earth's orbit: Pacemaker of the ice ages. *Science* **194,** 1121–1132 (1976).
8. Bhatt, U. S. *et al.* Circumpolar arctic tundra vegetation change is linked to sea ice decline. *Earth Interact.* **14,** 1–20 (2010).
9. Zhou, L. *et al.* Variations in northern vegetation activity inferred from satellite data of vegetation index during 1981 to 1999. *J. Geophys. Res.* **106,** 20069–20083 (2001).
10. Beck, P. S. A. & Goetz, S. J. Satellite observations of high northern latitude vegetation productivity changes between 1982 and 2008: Ecological variability and regional differences. *Environ. Res. Lett.* **6,** 045501 (2011).
11. Forbes, B. C., Macias-Fauria, M. & Zetterberg, P. Russian Arctic warming and 'greening' are closely tracked by tundra shrub willows. *Glob. Change Biol.* **16,** 1542–1554 (2010).
12. Macias-Fauria, M., Forbes, B. C., Zetterberg, P. & Kumpula, T. Eurasian Arctic greening reveals teleconnections and the potential for structurally novel ecosystems. *Nature Clim. Change* **2,** 613–618 (2012).
13. Walker, M. D. *et al.* Plant community responses to experimental warming across the tundra biome. *Proc. Natl Acad. Sci. USA* **103,** 1342–1346 (2006).
14. Myers-Smith, I. H. *et al.* Shrub expansion in tundra ecosystems: Dynamics, impacts and research priorities. *Environ. Res. Lett.* **6,** 045509 (2011).
15. Callaghan, T. V., Tweedie, C. E. & Webber, P. J. Multi-decadal changes in tundra environments and ecosystems: The International Polar Year-Back to the Future Project (IPY-BTF). *Ambio* **40,** 555–557 (2011).

16. Peng, C. *et al.* A drought-induced pervasive increase in tree mortality across Canada's boreal forests. *Nature Clim. Change* **1,** 467–471 (2011).

17. Bokhorst, S. F., Bjerke, J. W., Tømmervik, H., Callaghan, T. V. & Phoenix, G. K. Winter warming events damage sub-Arctic vegetation: Consistent evidence from an experimental manipulation and a natural event. *J. Ecol.* **97,** 1408–1415 (2009).

18. Soja, A. J. *et al.* Climate-induced boreal forest change: Predictions versus current observations. *Glob. Planet. Change* **56,** 274–296 (2007).

19. Smith, L. C., Sheng, Y., MacDonald, G. M. & Hinzman, L. D. Disappearing Arctic Lakes. *Science* **308,** 1429–1429 (2005).

20. Smol, J. P. & Douglas, M. S. V. Crossing the final ecological threshold in high Arctic ponds. *Proc. Natl Acad. Sci. USA* **104,** 12395–12397 (2007).

21. Callaghan, T. V., Christensen, T. R. & Jantze, E. J. Plant and vegetation dynamics on Disko Island, west Greenland: snapshots separated by over 40 years. *Ambio* **40,** 624–637 (2011).

22. Klein, D. R. & Shulski, M. Lichen recovery following heavy grazing by reindeer delayed by climate warming. *Ambio* **38,** 11–16 (2009).

23. Bulygina, O. N., Groisman, P. Y., Razuvaev, V. N. & Korshunova, N. N. Changes in snow cover characteristics over Northern Eurasia since 1966. *Environ. Res. Lett.* **6,** 045204 (2011).

24. Euskirchen, E. S., McGuire, A. D. & Chapin, F. S. Energy feedbacks of northern high-latitude ecosystems to the climate system due to reduced snow cover during 20th century warming. *Glob. Change Biol.* **13,** 2425–2438 (2007).

25. Chapin, F. S. *et al.* Role of land-surface changes in Arctic summer warming. *Science* **310,** 657–660 (2005).

26. Sturm, M. *et al.* Winter biological processes could help convert arctic tundra to shrubland. *Bioscience* **55,** 17–26 (2005).

27. Toutoubalina, O. V. & Rees, W. G. Remote sensing of industrial impact on Arctic vegetation around Noril'sk, northern Siberia: Preliminary results. *Int. J. Remote Sensing* **20,** 2979–2990 (1999).

28. Tømmervik, H. *et al.* Above ground biomass changes in the mountain birch forests and mountain heaths of Finnmarksvidda, northern Norway, in the period 1957–2006. *Forest Ecol. Manage.* **257,** 244–257 (2009).

29. Olofsson, J., Tømmervik, H. & Callaghan, T. V. Vole and Lemming activity observed from space. *Nature Clim. Change* **2,** 880–883 (2012).

30. Riahi, K., Grübler, A. & Nakicenovic, N. Scenarios of long-term socio-economic and environmental development under climate stabilization. *Technol. For. Soc. Change* **74,** 887–935 (2007).

Acknowledgements

Author contributions

The analysis was performed by X.L., R.B.M, Z.Z and J.B. All authors contributed with ideas, writing and discussions.

Additional information

Supplementary information is available in the online version of the paper. Reprints and permissions information is available online at www.nature.com/reprints. Correspondence and requests for materials should be addressed to X.L or R.B.M.

Competing financial interests

The authors declare no competing financial interests.